J|A|C|S
ARTICLES
Published on Web 12/30/2003

Hyponitrite Radical, a Stable Adduct of Nitric Oxide and Nitroxyl

Gregory A. Poskrebyshev,[†,§] Vladimir Shafirovich,[‡] and Sergei V. Lymar*[,†]

Contribution from the Chemistry Department, Brookhaven National Laboratory, Upton, New York 11973, and Chemistry Department and Radiation and Solid State Laboratory, New York University, New York, New York 10003

Received August 20, 2003; E-mail: lymar@bnl.gov

Abstract: All major properties of the aqueous hyponitrite radicals ($ONNO^-$ and ONNOH), the adducts of nitric oxide (NO) and nitroxyl ($^3NO^-$ and ^1HNO), are revised. In this work, the radicals are produced by oxidation of various hyponitrite species in the 2−14 pH range with the OH, N_3, or SO_4^- radicals. The estimated rate constants with OH are 4×10^7, 4.2×10^9, and 8.8×10^9 M^{-1} s^{-1} for oxidations of HONNOH, $HONNO^-$, and $ONNO^{2-}$, respectively. The rate constants for $N_3 + ONNO^{2-}$ and $SO_4^- + HONNO^-$ are 1.1×10^9 and 6.4×10^8 M^{-1} s^{-1}, respectively. The $ONNO^-$ radical exhibits a strong characteristic absorption spectrum with maxima at 280 and 420 nm ($\epsilon_{280} = 7.6 \times 10^3$ and $\epsilon_{420} = 1.2 \times 10^3$ M^{-1} cm^{-1}). This spectrum differs drastically from those reported, suggesting the radical misassignment in prior work. The ONNOH radical is weakly acidic; its pK_a of 5.5 is obtained from the spectral changes with pH. Both $ONNO^-$ and ONNOH are shown to be over 3 orders of magnitude more stable with respect to elimination of NO than it has been suggested previously. The aqueous thermodynamic properties of $ONNO^-$ and ONNOH radicals are derived by means of the gas-phase ab initio calculations, justified estimates for ONNOH hydration, and its pK_a. The radicals are found to be both strongly oxidizing, $E°(ONNO^-/ONNO^{2-}) = 0.96$ V and $E°$(ONNOH, H^+/HONNOH) = 1.75 V, and moderately reducing, $E°(2NO/ONNO^-) = -0.38$ V and $E°(2NO, H^+/ONNOH) = -0.06$ V, all vs NHE. Collectively, these properties make the hyponitrite radical an important intermediate in the aqueous redox chemistry leading to or originating from nitric oxide.

Introduction

The hyponitrite anion ($N_2O_2^{2-}$) and its conjugate acids (Figure 1) are the long-known metastable compounds with nitrogen in the +1 oxidation state. Their chemistry has been extensively studied and reviewed.[1] Alkali metal salts of only *trans*-hyponitrite have been prepared, and only the trans forms persist in aqueous solution; the cis forms are believed to be extremely unstable with respect to elimination of N_2O, e.g.,

$$HN_2O_2^- \rightarrow N_2O + OH^- \qquad (1)$$

Among the trans forms, the monoprotonated anion is the least stable, undergoing reaction 1 with an ~16 min half-life at 25 °C; the acid decays orders of magnitude more slowly, and the dianion hardly decays at all.[2,3] The one-electron oxidations of the various hyponitrite species should generate the hyponitrite radicals (HN_2O_2 and $N_2O_2^-$), as shown in Figure 1. Surprisingly, these reactions and the radicals so produced have never been explored with time-resolved techniques.

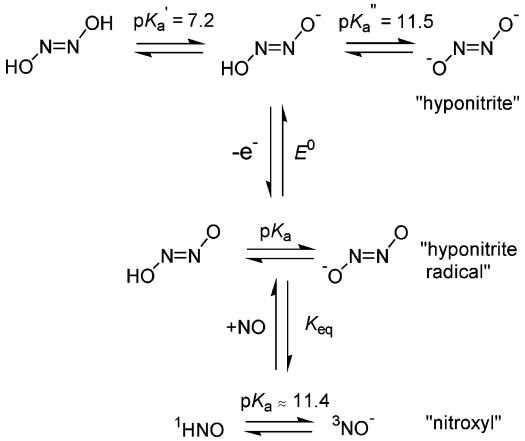

Figure 1. Relationship between hyponitrite, nitroxyl, nitric oxide, and the hyponitrite radical. The pK_a values for the hyponitrite species are from the review by Bonner and Hughes,[1] and the pK_a for nitroxyl is from Shafirovich and Lymar.[4] The values for $E°$, K_{eq}, and pK_a of HN_2O_2 will be evaluated in this work.

The existence of $N_2O_2^-$ was first postulated in the early 1970s by two research groups dealing with the pulse radiolysis of aqueous nitric oxide (NO).[5−7] The very rapid scavenging of the H atoms and the hydrated electrons by NO was used to generate the nitroxyl species (HNO/NO^-) and the intense absorption spectrum with a maximum around 380 nm (Figure 2, spectrum

[†] Brookhaven National Laboratory.
[‡] New York University.
[§] On leave from the Institute of Energy Problems of Chemical Physics, Russian Academy of Sciences, Moscow 117829, Russia.

(1) Bonner, F. T.; Hughes, M. N. *Comments Inorg. Chem.* **1988**, *7*, 215−234.
(2) Hughes, M. N.; Stedman, G. *J. Chem. Soc.* **1963**, 1239−1243.
(3) Buchholz, J. R.; Powell, R. E. *J. Am. Chem. Soc.* **1963**, *85*, 509−511.

10.1021/ja038042l CCC: $27.50

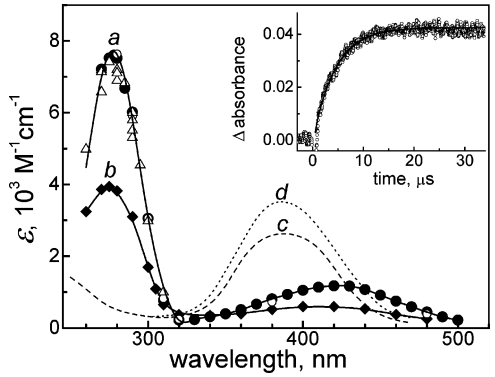

Figure 2. Absorption spectra of transients obtained via oxidation of hyponitrite (a and b) in N_2O-satutated solutions at radiation doses in the 1.5−6 Gy range (1−4 μM of total radicals from water radiolysis). At wavelengths below 290 nm, the experimental transient spectra have been corrected for bleaching due to consumption of the initial hyponitrite species. Spectrum a is assigned to the $N_2O_2^-$ radical produced by hyponitrite oxidation with OH at pH 12−12.5 (●, 1−2 mM $N_2O_2^{2-}$ in NaOH) and at pH 9.5 (△, 0.27 mM $HN_2O_2^-$ in 20 mM borate) and with N_3 at pH 12 (○, 10 mM N_3^- plus 1 mM $N_2O_2^{2-}$ in NaOH). Spectrum b (◆) is assigned to the HN_2O_2 radical produced by hyponitrous acid oxidation with OH at pH 3 (1−2 mM $H_2N_2O_2$ in $HClO_4$). Spectra c and d are adapted from Seddon and co-workers[7] and have been attributed to the $N_2O_2^-$ radical and $N_3O_3^-$ anion, respectively, by these and the other[5] authors. The inset shows a typical transient absorption growth kinetics recorded at 290 nm in a 2 mM $N_2O_2^{2-}$ solution at pH 13.7; the solid line gives an exponential fit to the data.

c) appearing shortly after the radiation pulse was attributed to the $N_2O_2^-$ radical produced in the reversible addition reaction

$$NO^- + NO \leftrightarrows N_2O_2^- \qquad (2)$$

The protonated form of NO^- (HNO, with the H atom on the N atom) reportedly reacted in a similar manner with an identical forward rate constant. The data interpretation was complicated by the addition of a second NO, yielding the $N_3O_3^-$ anion, which then slowly decomposed to nitrous oxide and nitrite

$$N_2O_2^- + NO \rightarrow N_3O_3^- \rightarrow N_2O + NO_2^- \qquad (3)$$

Surprisingly, the spectra assigned to $N_2O_2^-$ and $N_3O_3^-$ were essentially the same, differing only slightly in intensities (compare spectra c and d in Figure 2). However, it appears highly unlikely that these species, one radical and the other closed-shell molecule with differing atomic composition, should exhibit such a striking spectral similarity. The $N_3O_3^-$ spectrum has been confirmed by more recent studies,[4,8] but the $N_2O_2^-$ spectral assignment remains questionable. The original evidence supporting the assignment was indirect and relied on a quantitative description of the postulated mechanism for radiolysis of aqueous NO.

One highly unusual complication that has not been recognized in the early pulse radiolysis work is that HNO and NO^- have different spin multiplicities in their ground states. While HNO is a singlet, the conjugate NO^- anion, which is isoelectronic with molecular oxygen and possesses the same HOMO degeneracy, has a triplet ground state.[4,9−11] As a result, the H + NO and the e_{aq}^- + NO reaction should generate ^{1}HNO and $^3NO^-$, respectively. Recent reports have placed the pK_a of ^{1}HNO at ~11.4,[4,10] i.e., about 7 units higher than the previously accepted value of 4.7 based on the early pulse radiolysis work,[5] and have shown that the spin-forbidden protic equilibration of these species (Figure 1) occurs rather slowly.[4,11] In addition, ^{1}HNO and $^3NO^-$ have been found to exhibit markedly different reactivities toward NO,[4,11] also contrary to the conclusions of the pulse radiolysis studies. Thus, both the mechanism of pulse radiolysis suggested in earlier work and the description of the $N_2O_2^-$ radical based on this mechanism require revision.

Interest in properties and the reactivity of the hyponitrite radical arises from the likelihood of its intermediacy in both biological and environmental redox processes that involve NO. The $N_2O_2^-$ radical (either free or metal-coordinated) is expected to intervene when the nitroxyl species are generated in the NO-containing environments (reaction 2 and its analogues with HNO and metal-coordinated HNO or NO^-).[12,13] In turn, the nitroxyl species can be produced en route to NO from arginine, during denitrification (reduction of nitrate to N_2O and/or N_2), and as the intermediates of NO metabolism. These possibilities have engendered a rapidly growing interest in the biological roles of nitroxyl, and a number of research groups have been recently involved in the related studies mainly employing Angeli's salt for slow release of nitroxyl into various environments.[14] The mechanistic interpretations of observed effects require a detailed knowledge of the underlying chemistry of nitroxyl and species derived from it; prominent among them is the hyponitrite radical. In this study, we use pulse radiolysis and flash photolysis to generate the hyponitrite radicals from hyponitrite at the 2−14 pH range and investigate their properties. The radical absorption spectrum is found to be entirely different from that described previously, suggesting that it has been misassigned in the prior studies.[5,7] The radical energetics, redox properties, acidity, and stability with respect to dissociation into nitric oxide and nitroxyl are all extensively revised.

Experimental Section

Sample Solutions. Analytical grade buffers, $HClO_4$, and NaOH and Milli-Q purified (ASTM type I) water were used throughout. Sodium *trans*-hyponitrite ($Na_2N_2O_2 \cdot xH_2O$, from Aldrich) was used as received. Its alkaline (pH 12−13) or acidic (pH 2−3) stock solutions were prepared daily and kept on ice. The hyponitrite concentrations were

(4) Shafirovich, V.; Lymar, S. V. *Proc. Natl. Acad. Sci. U.S.A.* **2002**, *99*, 7340−7345.
(5) Grätzel, M.; Taniguchi, S.; Henglein, A. *Ber. Bunsen-Ges. Phys. Chem.* **1970**, *74*, 1003−1010.
(6) Seddon, W. A.; Young, M. J. *Can. J. Chem.* **1970**, *48*, 393−394.
(7) Seddon, W. A.; Fletcher, J. W.; Sopchyshyn, F. C. *Can. J. Chem.* **1973**, *51*, 1123−1130.
(8) Czapski, G.; Holcman, J.; Bielski, B. H. J. *J. Am. Chem. Soc.* **1994**, *116*, 11465−11469.
(9) Bartberger, M. D.; Fukuto, J. M.; Houk, K. N. *Proc. Natl. Acad. Sci. U.S.A.* **2001**, *98*, 2194−2198.
(10) Bartberger, M. D.; Liu, W.; Ford, E.; Miranda, K. M.; Switzer, C.; Fukuto, J. M.; Farmer, P. J.; Wink, D. A.; Houk, K. N. *Proc. Natl. Acad. Sci. U.S.A.* **2002**, *99*, 10958−10963.
(11) Shafirovich, V.; Lymar, S. V. *J. Am. Chem. Soc.* **2003**, *125*, 6547−6552.
(12) Bazylinski, D. A.; Hollocher, T. C. *Inorg. Chem.* **1985**, *24*, 4285−4288.
(13) (a) MacNeil, J. H.; Berseth, P. A.; Bruner, E. L.; Perkins, T. L.; Wadia, Y.; Westwood, G.; Trogler, W. C. *J. Am. Chem. Soc.* **1997**, *119*, 1668−1675. (b) Franz, K. J.; Lippard, S. J. *J. Am. Chem. Soc.* **1998**, *120*, 9034−9040. (c) Bayachou, M.; Lin, R.; Cho, W.; Farmer, P. J. *J. Am. Chem. Soc.* **1998**, *120*, 9888−9893.
(14) (a) Liochev, S. I.; Fridovich, I. *Free Radical Biol. Med.* **2003**, *34*, 1399−1404. (b) Miranda, K. M.; Paolocci, N.; Katori, T.; Thomas, D. D.; Ford, E.; Bartberger, M. D.; Espey, M. G.; Kass, D. A.; Feelisch, M.; Fukuto, J. M.; Wink, D. A. *Proc. Natl. Acad. Sci. U.S.A.* **2003**, *100*, 9196−9201. (c) Cook, N. M.; Shinyashiki, M.; Jackson, M. I.; Leal, F. A.; Fukuto, J. M. *Arch. Biochem. Biophys.* **2003**, *410*, 89−95. (d) Ivanova, J.; Salama, G.; Clancy, R. M.; Schor, N. F.; Nylander, K. D.; Stoyanovsky, D. A. *J. Biol. Chem.* **2003**, *278*, 42761−42768. (e) Ohshima, H.; Tatemichi, M.; Sawa, T. *Arch. Biochem. Biophys.* **2003**, *417*, 3−11. (f) Kaur, H.; Hughes, M. N.; Green, C. J.; Naughton, P.; Foresti, R.; Motterlini, R. *FEBS Lett.* **2003**, *543*, 113−119. (g) Naughton, P.; Foresti, R.; Bains, S. K.; Hoque, M.; Green, C. J.; Motterlini, R. *J. Biol. Chem.* **2002**, *277*, 40666−40674.

assayed spectrophotometrically at the 248 nm absorption maximum of $N_2O_2^{2-}$ using $\epsilon_{248} = 6550\ M^{-1}\ cm^{-1}$;[15] the concentrations so obtained and the analysis for Na using AA spectroscopy corresponded to 3.0 ± 0.2 molecules of H_2O per $Na_2N_2O_2$ in the commercial salt. An aliquot of the stock was diluted to the desired pH, saturated with either Ar or N_2O, and used for pulse radiolysis experiments within 1 h.

Kinetic Measurements. The pulse radiolysis was carried out with 2 meV electrons from a van de Graaff accelerator; pulse widths were in the range 0.06−0.8 μs. Either one or three passes of analyzing light through a 2 cm cell were used in the detection optical path. For the kinetics recorded on a time scale of less than 100 μs, the analyzing Xe-arc light source was pulsed. All experiments were done with temperature stabilization at 25 ± 0.5 °C. The yields of primary radicals from water radiolysis (in number of radicals per 100 eV) were taken as $G(OH) = 2.8$, $G(e_{aq}^-) = 2.8$, and $G(H) = 0.6$ in Ar-purged solutions and $G(OH) = 6.1$ and $G(H) = 0.6$ in N_2O-saturated solutions. Dosimetry was performed with an N_2O-saturated 10 mM KSCN solution using $G\epsilon = 4.87 \times 10^4$ ions $(100\ eV)^{-1}\ M^{-1}\ cm^{-1}$ for the $(SCN)_2^-$ radical at 472 nm.

Flash photolysis was done under Ar atmosphere in a flow cell, as described elsewhere.[4,11] An alkaline solution of $N_2O_2^{2-}$ was mixed with buffer also containing $S_2O_8^{2-}$ prior to entering the cell. A 308 nm excimer laser was employed to cleave $S_2O_8^{2-}$ into a pair of SO_4^- radicals, which then were used to oxidize hyponitrite.

Ab initio calculations of the thermochemistry were performed with Gaussian 98 using the complete basis set method (CBS-Q);[16] the results are reported for 298 K.

Results

Formation and Spectra. Pulse radiolysis of aqueous $N_2O_2^{2-}$ provides a convenient method to generate the hyponitrite radical. All three primary radicals from water radiolysis (OH, e_{aq}^-, and H) can be employed for this purpose in alkaline N_2O-saturated solution, where e_{aq}^- and H are rapidly converted into OH through the reactions

$$H + OH^- \rightarrow e_{aq}^- + H_2O$$
$$k_4 = 2.4 \times 10^7\ M^{-1}\ s^{-1}\ ^{17} \qquad (4)$$

$$e_{aq}^- + N_2O + H_2O \rightarrow N_2 + OH^- + OH$$
$$k_5 = 9.1 \times 10^9\ M^{-1}\ s^{-1}\ ^{18} \qquad (5)$$

In alkali, the OH radical is in equilibrium with its conjugate base

$$OH \leftrightarrows H^+ + O^- \qquad pK_6 = 11.7^{19} \qquad (6)$$

In the presence of $N_2O_2^{2-}$, a new and relatively long-lived transient absorption appears throughout the most of the UV−visible spectral region shortly after the radiation pulse; the fully developed absorption spectrum is plotted in Figure 2 (spectrum a), and the inset shows its typical growth kinetics. The growth is wavelength independent and exponential, with the first-order

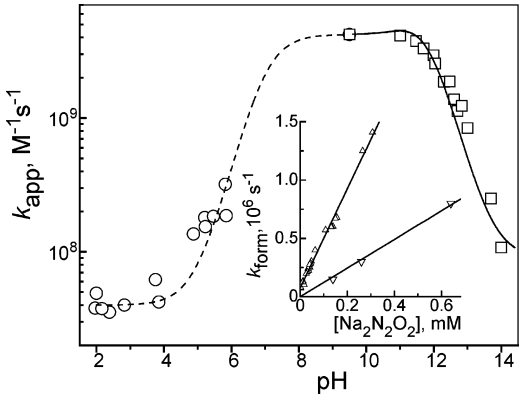

Figure 3. Dependence upon pH of the apparent bimolecular rate constant, k_{app}, for the formation of hyponitrite radical through reactions 7, 8, 11, 12, and 17 in N_2O-saturated solutions. (□) Alkaline region, the solid curve corresponds to eq 13. (○) Acidic region, the dashed curve corresponds to eq 20 (see text for equation parameters that were used). The inset shows typical dependencies upon added hyponitrite of the first-order rate constant, k_{form}, for $N_2O_2^-$ accumulation observed at 290 nm. (△) At pH 9.2−9.5 in 20 mM borate; hyponitrite is predominantly present as $HN_2O_2^-$. (▽) At pH 12.8 in NaOH; hyponitrite is predominantly present as $N_2O_2^{2-}$. The solid lines give linear fits to the data that were used for computing the k_{app} values.

formation rate constant, k_{form}, proportional to the concentration of $N_2O_2^{2-}$ (Figure 3, inset). We thus attribute this spectrum to the $N_2O_2^-$ radical produced in the reactions with both acidic and basic forms of hydroxyl radical

$$N_2O_2^{2-} + OH \rightarrow N_2O_2^- + OH^- \qquad (7)$$

$$N_2O_2^{2-} + O^- + H_2O \rightarrow N_2O_2^- + 2OH^- \qquad (8)$$

The molar absorptivities for the $N_2O_2^-$ spectrum in Figure 2 have been computed assuming complete conversion of all radicals, that is by taking the radiation yield $G(N_2O_2^-) = 6.7$ radicals per 100 eV in N_2O-saturated alkaline solution. This spectrum cannot be assigned to an adduct of $N_2O_2^{2-}$ and OH/O^- because the same spectrum is obtained in the presence of excess sodium azide (Figure 2), where all OH radicals are first converted into the strongly oxidizing azide radical, which then reacts with $N_2O_2^{2-}$

$$N_3^- + OH \rightarrow N_3 + OH^- \qquad (9)$$

$$N_2O_2^{2-} + N_3 \rightarrow N_2O_2^- + N_3^- \qquad (10)$$

The rate constant $k_{10} = 1.1 \times 10^9\ M^{-1}\ s^{-1}$ has been determined in 20 mM NaOH from the concentration dependence of the $N_2O_2^-$ formation rate (for details, see Supporting Information Figure S2).

The transient spectrum is unchanged upon lowering pH to 9.5, where $HN_2O_2^-$ is the dominant form of hyponitrite (Figure 2). We therefore assign the transient formation at this pH to the reaction

$$HN_2O_2^- + OH \rightarrow N_2O_2^- + H_2O \qquad (11)$$

The rate of $N_2O_2^-$ formation becomes much larger than that in strongly alkaline solutions as seen from the slopes of the concentration dependencies of k_{form} in Figure 3, inset. Measurements of such dependencies in the pH range 7−11 are complicated by the relatively rapid decomposition of $HN_2O_2^-$.

(15) Polydoropoulos, C. N.; Voliotis, S. D. *Anal. Chim. Acta* **1968**, *40*, 170−172.

(16) Frisch, M. J.; Trucks, G. W.; Schlegel, H. B.; Scuseria, G. E.; Robb, M. A.; Cheeseman, J. R.; Zakrzewski, V. G.; Montgomery, J. A.; Stratmann, R. E.; Burant, J. C.; Dapprich, S.; Millam, J. M.; Daniels, A. D.; Kudin, K. N.; Strain, M. C.; Farkas, O.; Tomasi, J.; Barone, V.; Cossi, M.; Cammi, R.; Mennucci, B.; Pomelli, C.; Adamo, C.; Clifford, S.; Ochterski, J.; Petersson, G. A.; Ayala, P. Y.; Cui, Q.; Morokuma, K.; Malick, D. K.; Rabuck, A. D.; Raghavachari, K.; Foresman, J. B.; Cioslowski, J.; Ortiz, J. V.; Stefanov, B. B.; Liu, G.; Liashenko, A.; Piskorz, P.; Komaromi, I.; Gomperts, R.; Martin, R. L.; Fox, D. J.; Keith, T.; Al-Laham, M. A.; Peng, C. Y.; Nanayakkara, A.; Gonzalez, C.; Challacombe, M.; Gill, P. M. W.; Johnson, B. G.; Chen, W.; Wong, M. W.; Andres, J. L.; Head-Gordon, M.; Replogle, E. S.; Pople, J. A. *Gaussian 98*, revision A.7; Gaussian, Inc.: Pittsburgh, PA, 1998.

Importantly, the decomposition does not result in solution contamination, for it stoichiometrically generates N_2O (reaction 1),[1,12,20] which is already present in the solution at a saturating level. In agreement with published results,[2] we have found that the decomposition is strictly exponential with a 16.3 min half-life at pH 9.2 and 25 ± 0.1 °C. This feature has afforded accurate assessment of the $HN_2O_2^-$ concentration at the moment of pulse radiolysis run by registering the time elapsed since an aliquot of hyponitrite has been added to the buffer.

As shown in Figure 2, the apparent second-order rate constant, k_{app}, for hyponitrite oxidation with hydroxyl radical is strongly pH dependent; the k_{app} values have been obtained from concentration dependencies such as those in the figure inset. The pH dependence of k_{app} is expected, as four acid−base forms of the reagents are involved, and the reaction

$$HN_2O_2^- + O^- \rightarrow N_2O_2^- + OH^- \qquad (12)$$

should also be considered along with reactions 7, 8, and 11. In the pH range 9−14, the predicted pH dependence is given by the equation

$$k_{app} = \frac{k_{11}[H^+]^2 + (k_7 + k_{12}K_6/K_a'')K_a''[H^+] + k_8K_a''K_6}{(K_a'' + [H^+])(K_6 + [H^+])} \qquad (13)$$

which can be well fitted to the data with $pK_a'' = 11.5$, $pK_6 = 11.7$ and $k_{11} = 4.2 \times 10^9$, $k_7 + k_{12}K_6/K_a'' = 9.0 \times 10^9$, and $k_8 = 9.0 \times 10^7$ M^{-1} s^{-1} (Figure 3). The proton ambiguity in reactions 7 and 12 does not allow separation of their rate constants without invoking extrakinetic considerations. One can estimate an upper limit for k_{12} from the analogous $HO_2^- + O^-$ reaction, which also occurs by H-atom abstraction and should be more energetically favorable. The latter reaction has the rate constant of 4×10^8 M^{-1} s^{-1};[18] assuming the same value for k_{12}, we obtain $k_7 \approx 8.8 \times 10^9$ M^{-1} s^{-1} and suggest this number as the best estimate. Reaction 12 thus becomes practically inconsequential. These estimates appear reasonable, because we expect that (i) $k_7 > k_{11}$, a trend typical of the oxidations by OH of various substrates,[18] and (ii) $k_7 > k_{12}$, for reaction 7 is slightly more exothermic than reaction 12 ($pK_6 > pK_a''$) and there is an unfavorable Coulombic factor for the latter.

In acidic solutions, reaction 4 plays no role and reaction 5 is in competition with rapid scavenging of e_{aq}^- by the hydrogen ions

$$e_{aq}^- + H^+ \rightarrow H \qquad k_{14} = 2.3 \times 10^{10}\ M^{-1}\ s^{-1}\ [18] \qquad (14)$$

At pH 3, most of hydrated electrons still react with N_2O and the radiation yield of OH is about 5.4 radicals per 100 eV, which is only 20% lower than in N_2O-saturated alkaline solution. However, the transient absorption spectra differ strongly (compare spectra a and b in Figure 2); the spectrum in acid appears to be slightly blue-shifted and is considerably weaker than the spectrum in base. Such a spectral change is indicative of the protonation of $N_2O_2^-$, i.e., the equilibrium

$$HN_2O_2 \leftrightarrows H^+ + N_2O_2^- \qquad pK_{15} \qquad (15)$$

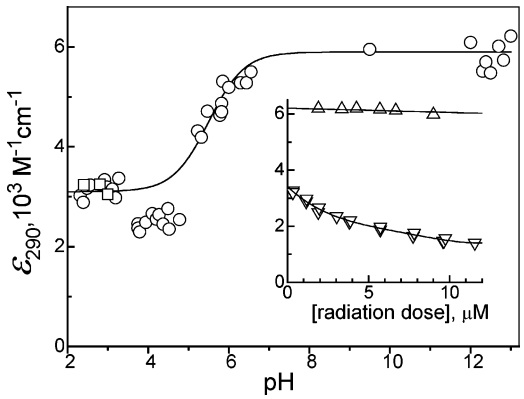

Figure 4. Dependence upon pH of the apparent molar absorptivity at 290 nm of the hyponitrite radical. (○) In N_2O-saturated solution; the radical radiation yields were taken as $G(OH) + G(H) = 6.7$ radicals per 100 eV at pH < 5 and pH ≥ 12 and $G(OH) = 6.1$ radicals per 100 eV at 5 < pH < 10. (□) In Ar-saturated solution; the radical radiation yield was taken as $G(OH) + G(e_{aq}^-) + G(H) = 6.2$ radicals per 100 eV, as explained in the text. The solid line corresponds to eq 16 with $pK_{15} = 5.5$. The inset shows typical dependencies of the apparent molar absorptivities upon the radiation dose expressed in μM of the hyponitrite radicals generated per radiation pulse. (△) At pH 13 in 2mM $N_2O_2^{2-}$; (▽) at pH 3 in 2.1 mM $H_2N_2O_2$. The "true" ϵ_{290} values plotted for various pH's have been obtained by extrapolating the corresponding dose dependencies to zero doses.

A similar spectral change occurs upon the protonation of $N_2O_2^{2-}$ (Supporting Information Figure S1). The pH dependence of the apparent molar absorptivity of the radical measured at 290 nm (Figure 4) has a typical appearance of a titration curve and, for the most part, conforms to the equation

$$\epsilon_{290} = \frac{\epsilon_{290}(N_2O_2^-)K_{15} + \epsilon_{290}(HN_2O_2)[H^+]}{K_{15} + [H^+]} \qquad (16)$$

where $\epsilon_{290}(N_2O_2^-)$ and $\epsilon_{290}(HN_2O_2)$ are molar absorptivities of the radical's basic and acidic forms. As seen in Figure 4, the inflection point in the pH profile corresponds to $pK_{15} = 5.5$ and the acidic form dominates below pH 4.

Only a small (≈10%) decrease in the transient absorption amplitude has occurred when N_2O was replaced by argon at a pH around 3, in which case essentially all hydrated electrons are converted to H by reaction 14 and the radiation yield of OH is reduced 2-fold compared with that of an N_2O-saturated solution (i.e., it becomes lower than the H yield). As hyponitrite is fully protonated at pH 3, this observation suggests that both OH and H are capable of generating the HN_2O_2 radical from $H_2N_2O_2$. Accordingly, when the molar absorptivity of HN_2O_2 is calculated by taking its radiation yield $G(HN_2O_2) = G(OH) + G(e_{aq}^-) + G(H)$, values essentially identical to those measured in an N_2O-saturated solution are obtained (Figure 4). The oxidation by OH is believed to occur via H-atom abstraction

$$H_2N_2O_2 + OH \rightarrow HN_2O_2 + H_2O \qquad (17)$$

while for the H atom we consider two possibilities. One also involves H-atom abstraction

$$H_2N_2O_2 + H \rightarrow HN_2O_2 + H_2 \qquad (18)$$

and the other generates OH radical

$$H_2N_2O_2 + H \rightarrow H_2O + N_2 + OH \qquad (19)$$

(17) Han, P.; Bartels, D. M. *J. Phys. Chem.* **1990**, *94*, 7294−7299.
(18) Buxton, G. V.; Mulazzani, Q. G.; Ross, A. B. *J. Phys. Chem. Ref. Data* **1995**, *24*, 1055−1349.

which then engages in reaction 17. The latter pathway is reminiscent of the N_2O reduction in reaction 5; indeed, N_2O can be properly considered as an anhydride of $H_2N_2O_2$. As discussed next, the kinetic data for acidic solution are more suggestive of reaction 19 than reaction 18.

The apparent second-order rate constant for formation of the transient species in acidic solutions is about 2 orders of magnitude smaller than at pH 9.5 (Figure 3). In an N_2O-saturated solution at pH 3−4, this rate constant is mainly due to reaction 17 and so $k_{17} \approx 4 \times 10^7$ M^{-1} s^{-1}. With Ar-saturation at around pH 2−3, the H atom contributes about 50% to the formation of HN_2O_2, and yet no biphasic behavior in the HN_2O_2 accumulation kinetics due to the parallel occurrence of reactions 17 and 18 has been observed. If reaction 18 were the predominant pathway for H, this result would indicate that k_{18} is coincidentally nearly identical to k_{17}, which is unlikely as reaction 17 is much more energetically favorable than reaction 18. A more reasonable interpretation is that the very exothermic reaction 19 is the main pathway for H atom disappearance and that it is at least several times more rapid than reaction 17. Then the OH radical would be the only oxidant present in solution shortly after the radiation pulse. Considering only reactions 11 and 17 in the pH range 2−9, the pH dependence of k_{app} can be described by the following equation

$$k_{app} = \frac{k_{11}K'_a + k_{17}[H^+]}{K'_a + [H^+]} \qquad (20)$$

which is plotted as the dashed line in Figure 3 with $pK'_a = 7.2$, $k_{11} = 4.2 \times 10^9$ M^{-1} s^{-1}, and $k_{17} = 4 \times 10^7$ M^{-1} s^{-1}. As used here, eqs 13, 16, and 20 are only approximate because the pK_a values involved and some rate constants depend on the solution ionic strength and these dependencies are not known. Nonetheless, these equations satisfactorily reproduce the observed wide-range pH profiles for both ϵ_{290} and k_{app}, with the exception of the pH region 4−5 in the former, where the observed ϵ_{290} values are ~20% lower than predicted by eq 16. We attribute this deviation to a small contamination of $H_2N_2O_2$ solutions with the nitrite anion, whose reaction with OH is about 250 times faster than that of $H_2N_2O_2$ and results in the loss of oxidant. This rate comparison suggests that even about a 0.1% nitrite contamination in hyponitrite would be sufficient to account for the data deviation at pH 4−5 in Figure 4. At and below pH 3, nitrite is mostly protonated ($pK_a(HNO_2) = 3.2$) and should contribute negligibly to the loss of OH; similar arguments hold for pH > 5, where OH reactivity is dominated by its rapid reaction with $HN_2O_2^-$ (reaction 11). Some nitrite contamination in acidic hyponitrite is practically unavoidable because nitrite is among the products of $H_2N_2O_2$ decomposition, which is a slow, erratic, and poorly understood process reportedly involving free radical chain reactions.[3,21]

As shown in the inset to Figure 4, the apparent molar absorptivities decrease with radiation dose and this effect is more pronounced in the acidic medium. This type of dependence is commonly observed in radiation chemistry and is attributable to the partial loss of oxidant due to diffusion-controlled cross- and self-recombinations of H and OH. As expected, the decrease of apparent ϵ_{290} with dose is steeper in the acidic solution, where the rate of hyponitrite oxidation by these radicals is much lower (Figure 3). A conventional procedure of extrapolating the dose dependence to zero dose has been employed in this work to obtain the pH dependence of ϵ_{290} in Figure 4.

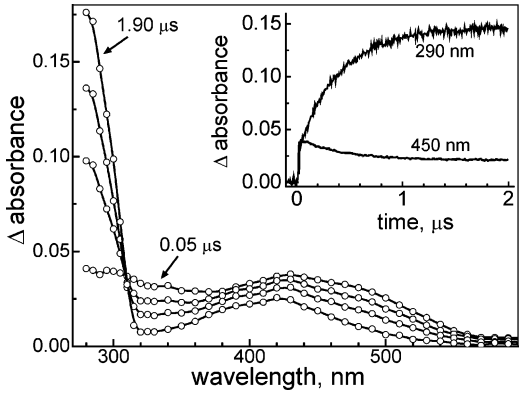

Figure 5. Transient absorption spectra measured at 0.05, 0.25, 0.50, and 1.90 μs after laser flash photolysis of Ar-purged solution containing 50 mM persulfate and 6.6 mM hyponitrite at pH 7.2 (0.1 M phosphate). The inset shows kinetic traces recorded at 290 nm ($N_2O_2^-$ accumulation) and 450 nm (SO_4^- decay).

The hyponitrite radical can also be obtained with the SO_4^- radical as an oxidant. The latter is conveniently generated by the photochemical cleavage of $S_2O_8^{2-}$ using laser flash photolysis. The transient absorption spectra recorded in Figure 5 correspond to the reaction

$$HN_2O_2^- + SO_4^- \rightarrow N_2O_2^- + SO_4^{2-} + H^+ \qquad (21)$$

Indeed, the spectra exhibit an isosbestic point around 310 nm, and the decay of SO_4^- absorption around 450 nm ($\epsilon_{450} = 1600 \pm 100$ M^{-1} cm^{-1})[22] is concurrent with the growth of absorption in the near UV region. The relative amplitudes of the absorption changes at 290 and 450 nm (Figure 5, inset) are within 10% of those expected from the stoichiometry of reaction 21 and the molar absorptivities of $N_2O_2^-$ at these wavelengths in Figure 2 (spectrum a). The rate constant $k_{21} = 6.4 \times 10^8$ M^{-1} s^{-1} has been determined at pH 9.3 (0.1 M borate) from the dependence of $N_2O_2^-$ growth kinetics upon $[HN_2O_2^-]$ (for details, see Supporting Information Figure S2). In contrast, the oxidation of $H_2N_2O_2$ by SO_4^- attempted at pH ≈ 2.3 (up to 20 mM of $H_2N_2O_2$ in 0.01 N HSO_4^-/SO_4^{2-}) was too slow to be measured.

Stability and Energetics. It has been proposed[5,7] and since then widely accepted that the $N_2O_2^-$ radical rapidly attains equilibrium with its constituents, i.e., the reversible dissociation reaction

$$N_2O_2^- \leftrightharpoons NO + {}^3NO^- \qquad (22)$$

which is reverse reaction 2 reformulated to reflect the correct spin of the ground-state NO^-. However, the previously reported[5,7] dissociation rate constant of 6.6×10^4 s^{-1} and equilibrium constant of $(3.5-3.9) \times 10^{-5}$ M are both incompat-

(19) Average of the two most recently reported values. For $pK = 12.0$, see: Hickel, B.; Corfitzen, H.; Sehested, K. *J. Phys. Chem.* **1996**, *100*, 17186−17190. For $pK = 11.5$, see: Poskrebyshev, G. A.; Neta, P.; Huie, R. E. *J. Phys. Chem. A* **2002**, *106*, 11488−11491.
(20) Bonner, F. T.; Stedman, G. In *Methods in Nitric Oxide Research*; Feelisch, M., Stamler, J. S., Eds.; Wiley: Chichester, 1996; pp 3−18.
(21) Buchholz, J. R.; Powell, R. E. *J. Am. Chem. Soc.* **1965**, *87*, 2350−2353.
(22) McElroy, W. J. *J. Phys. Chem.* **1990**, *94*, 2435−2441.

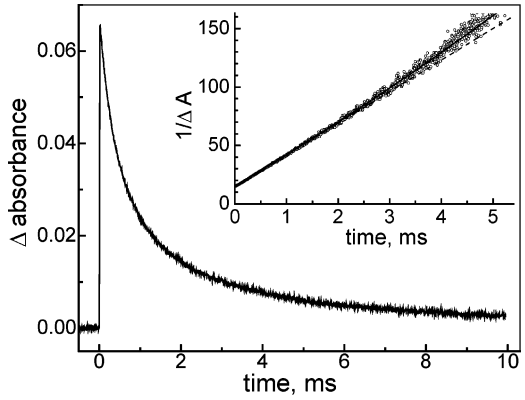

Figure 6. Typical kinetic trace for the decay of $N_2O_2^-$ recorded at 290 nm in an N_2O-saturated 0.1 M NaOH solution. The initial concentration of $N_2O_2^-$ is 5.5 μM. The inset shows the data in linear coordinates for the second-order reaction over 90% of the absorption decay. The dashed line corresponds to a purely bimolecular recombination with the rate constant of 1.6×10^8 M^{-1} s^{-1}, and the solid line is calculated with a 40 s^{-1} additional first-order decomposition pathway.

ible with our observations. Specifically, these numbers predict that equilibrium 22 is attained in about 15 μs and at a very low $N_2O_2^-$ concentration level without added NO. Under conditions of the inset in Figure 4, for example, the predicted fraction of undissociated $N_2O_2^-$ would be only 18% at a 10 μM dose and less than 3% at a 1 μM dose. Because neither $^3NO^-$ nor NO exhibit appreciable absorption around 290 nm,[4] one should expect a sharp decrease in apparent molar absorptivity toward lower doses, which is not observed. In fact, the slight opposite trend, whose origin has been mentioned above, is seen. In order for the $N_2O_2^-$ radical to remain over 90% undissociated in the 1−10 μM concentration range, the equilibrium constant K_{22} must be lower than 10^{-8} M. A similar situation exists with the HN_2O_2 radical dissociation

$$HN_2O_2 \leftrightarrows NO + HNO \qquad (23)$$

for which even larger rate (8×10^6 s^{-1})[7] and equilibrium (0.6×10^{-3} M [5] and 4.7×10^{-3} M [7]) constants have been ascribed. Clearly, we would not be able to observe the dose dependence in Figure 4 and to record the spectrum of HN_2O_2 in Figure 2 if these values were correct.

Additional strong evidence against rapid dissociation of the $N_2O_2^-$ radical comes from its decay kinetics; a typical absorption decay trace is shown in Figure 6. The kinetics is very close to purely second-order, suggesting the self-recombination

$$N_2O_2^- + N_2O_2^- \rightarrow \text{products} \qquad (24)$$

as the major pathway for the radical decay. A very good fit for about 85% of the decay can be obtained with a bimolecular rate constant of 1.6×10^8 M^{-1} s^{-1}. Only in the last 15% of the kinetics is a deviation from the second-order rate law discernible. Although small and comparable with the noise, the deviation is reproducible and consistent with the parallel occurrence of a first-order process. The average first-order rate constant of 40 ± 20 s^{-1} has been obtained from fitting 9 traces with various initial amplitudes to mixed first- and second-order kinetics. These results clearly show that dissociation of $N_2O_2^-$ cannot be rapid. Even though the $N_2O_2^-$ decay rate law is rather simple, its mechanism is complex and will be dealt with, along with other $N_2O_2^-$ reactions, in a forthcoming paper. Here, it is

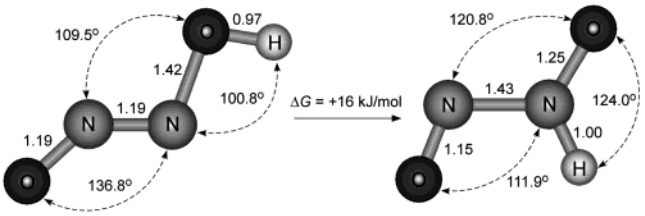

Figure 7. Lowest energy configurations for the gas-phase ONNOH and ONN(H)O isomers. Bond lengths are in angstroms, and the computed isomerization Gibbs energy is as shown.

sufficient to note that the bimolecular rate constant of 1.6×10^8 M^{-1} s^{-1} extracted from the decay kinetics is merely an observed parameter; it is proportional to but is not the actual rate constant for elementary reaction 24.

Since the reverse reactions 22 and 23 do occur,[4,5,7] the corresponding equilibria exist by virtue of microscopic reversibility. Recently Shafirovich and Lymar[4] have estimated $k_{-22} > 2 \times 10^9$ M^{-1} s^{-1}. Assuming for the sake of argument that the first-order component with a 40 s^{-1} rate constant in the $N_2O_2^-$ decay is entirely due to forward reaction 22 (which is not necessarily so), one estimates the upper limit for $K_{22} = k_{22}/k_{-22} < 2 \times 10^{-8}$ M, some 2000 times lower than the previously reported values. This result indicates that the dissociation is energetically significantly unfavorable.

To test this conclusion and to evaluate the reduction potentials of the hyponitrite radicals, we have resorted to ab initio (CBS-Q method) computations of energetics for the gas-phase species combined with reasonable assumptions about their energies of hydration. There exist two HN_2O_2 isomers with respect to the H atom position, the ONNOH and the ONN(H)O isomers shown in Figure 7. The calculated global energy minimum belongs to the former, as can be anticipated from the on the average larger O−H than N−H bond strength.[23] Both isomers are practically planar with the most stable trans configurations of the O atoms with respect to the N−N bond, but the energy differences with the corresponding lowest cis forms are small (for relative energies at various radical geometries, see Supporting Information note 1). One of the two previous calculations performed at a lower level gave the same geometries as have ours for the isomers in Figure 7,[24] while the other yielded insignificantly differing bonds and angles.[25] More surprising and contrary to the bond strength trend and to our results, both prior studies found a somewhat smaller enthalpy for ONN(H)O than for ONNOH. For the geometry in Figure 7, the absolute entropy $S°(ONNOH)_g = 277$ J/mol K of the O−H isomer and the enthalpy change $\Delta_{r25}H° = -227$ kJ/mol for its formation reaction

$$2NO(g) + H(g) \rightarrow \textit{trans}\text{-}ONNOH(g) \qquad (25)$$

have been computed. From these values and the experimental gas-phase data for NO and H in Table 1, the formation enthalpy $\Delta_fH°(ONNOH)_g = 172$ kJ/mol and free energy $\Delta_fG°(ONNOH)_g = 227$ kJ/mol are obtained.

(23) Huheey, J. E. *Inorganic Chemistry*, 3rd ed.; Harper & Row: New York, 1983.
(24) Mebel, A. M.; Morokuma, K.; Lin, M. C.; Melius, C. F. *J. Phys. Chem.* **1995**, *99*, 1900−1908.
(25) Bunte, S. W.; Rice, B. M.; Chabalowski, C. F. *J. Phys. Chem. A* **1997**, *101*, 9430−9438.

Table 1. Formation Energetics for Hyponitrite, Hyponitrite Radical, and Related Species[a]

species (phase)	$\Delta_f H°$ kJ/mol	$\Delta_f G°$ kJ/mol	$S°$ J/mol K	reference
ONNOH (g)	172	227	277	this work
ONNOH (aq)	125	210	177	this work
HONNOH (aq)	−64	41	174	this work[b]
H (g)	218	203	115	26
NO (g)	90	87	211	26
NO (aq)	na	102	na	27
^{1}HNO (aq)	na	115[c]	na	4
$^3NO^-$ (aq)	na	180[d]	na	4
$HONNO^-$ (aq)	−52	82	77	this work[b]
$ONNO^{2-}$ (aq)	−17	148	−27	this work[b]
$ONNO^-$ (aq)	na	241[e]	na	this work

[a] Standard states 1 atm in gas phase and 1 mol/kg in solution at 298 K; all values are rounded up to the nearest integer and "na" indicates nonavailable values. [b] For derivations, see Supporting Information note 2. [c] Stanbury[27] gives 109 kJ/mol. [d] Similar value of 175 kJ/mol is implied by $E°(NO/^3NO^-) = -0.76$ V obtained by Houk and co-workers[10] from ab initio calculations; the previous estimate of 64 kJ/mol by Stanbury[27] is believed to be incorrect. [e] Koppenol[28] calculated 141 kJ/mol based on $\Delta_f G°(^3NO^-) = 64$ kJ/mol[27] and $K_{22} = 3.9 \times 10^{-5}$ M;[7] both values are now believed to be incorrect.

Table 2. Hydration Energetics for Small and Medium Size Neutral Monohydroxy Compounds[a]

XOH species	$\Delta_{hyd}H°$ kJ/mol	$\Delta_{hyd}S°$ J/mol K	$\Delta_{hyd}G°$ kJ/mol	references
OOH	−49	−88	−22	29
ClOH	−49	−110	−16	30
ONOH	−41	−104	−10	31
ONOOH	−50[b]	−105	−18	32, 33, 26
H_3COH	−45	−107	−14	26
H_3COOH	−44[c]	−99	−14	34
HC(O)OH	−51	−96	−23	26, 35
$H_3CC(O)OOH$	−44[c]	−92	−17	34
average	−47	−100	−17	

[a] Standard states and rounding up as in Table 1. [b] Estimated using computed (CBS-QB3) gas-phase ΔH for $ONOOH = NO_2 + OH$,[33] tabulated $\Delta_f H°$ for NO_2 and OH,[26] and reported aqueous $\Delta_f H°(ONOOH)$.[32] [c] Corrected for sign error in original reference.

Collected in Table 2 are the hydration parameters for several small and medium size molecules that resemble the ONNOH radical; common among them is the presence of one terminal hydroxy group, i.e., the XOH compounds. The table shows that both the heat and entropy of hydration are confined to a narrow range of values despite significant variations in size and composition of the X moiety. The near constancy of $\Delta_{hyd}S°$ at about −100 J/mol K is expected; it has been noted before for a much wider range of small neutral species than shown in Table 2, including numerous compounds that do not bear terminal OH groups.[36] In contrast, the very small variability of $\Delta_{hyd}H°$ apparent in Table 2 is undoubtedly due mainly to this group, which always participates in three hydrogen bonds with water[37] and thereby dominates the heat of hydration. Based on Table 2, we can confidently set $\Delta_{hyd}G° = -17 \pm 7$ kJ/mol for the ONNOH radical and obtain an estimate $\Delta_f G°(ONNOH)_{aq} = 210$ kJ/mol for its aqueous free energy of formation, shown in Table 1 along with other formation parameters. It is more difficult to quantitatively assess hydration of the ONN(H)O radical isomer, because a representative dataset for its analogues is not available. However, one can reasonably assume somewhat weaker hydrogen bonding and a smaller attendant Gibbs energy of hydration for ONN(H)O (two H-bonds) than for ONNOH (three H-bonds). This should result in a larger energy gap between these two isomers in water than in gas phase. Because the $ONNO^-$ anion is the conjugate base of both protonated isomers, we expect pK_a(ONNOH) to be significantly larger than pK_a(ONN(H)O) and, thus, attribute $pK_{15} = 5.5$ determined from the data in Figure 4 to ONNOH. By means of this pK, we calculate $\Delta_f G°(ONNO^-)_{aq} = 241$ kJ/mol. Reassuringly, the relationship between the pK_a's of the two isomers of the protonated $ONNO^-$ radical is qualitatively the same as that for the isomers of the protonated ONO^{2-} radical; it was recently suggested that the O-bonded $ONOH^-$ isomer has a pK_a that is several units higher than that of the N-bonded $ON(H)O^-$ isomer.[38]

It is difficult to place with complete confidence an uncertainty on $\Delta_f G°(ONNO^-)_{aq}$ derived through the multistep procedure described above, but ±10 kJ/mol appears tenable. Using the previously evaluated (Table 1) free energies of formation for the aqueous products of $ONNO^-$ dissociation, the equilibrium constant for reaction 22 can be estimated as lying between 1×10^{-9} and 4×10^{-6} M. The lower number is consistent with the experimental upper limits for K_{22} obtained from Figures 4 and 6, but the higher number is not. Nonetheless, even this number is an order of magnitude below the K_{22} values suggested previously.

With the data in Table 1, the standard one-electron reduction potentials for the hyponitrite radical

$$\text{hyponitrite radical} + e^- \leftrightarrows \text{hyponitrite} \qquad (26)$$

can be estimated as $E°(N_2O_2^-/N_2O_2^{2-}) = 0.96$ V and $E°(HN_2O_2, H^+/H_2N_2O_2) = 1.75$ V, both vs NHE. If the uncertainties in $\Delta_f G°$ for both the hyponitrite radical and the hyponitrite species in Table 1 are indeed about 10 kJ/mol, these potentials should be accurate to ±0.15 V. Taking into account the pK_a values for the radical and hyponitrite species, the midpoint potential shown in Figure 8 is obtained at various pH values. It is evident that the radical should be quite strongly oxidizing, particularly in neutral and acidic media. At the same time, the radical can act as reductant, i.e., the electrode reaction

$$\text{hyponitrite radical} \leftrightarrows 2NO(aq) + e^- \qquad (27)$$

for which the standard potentials are $E°(2NO/N_2O_2^-) = -0.38$ V and $E°(2NO, H^+/HN_2O_2) = -0.06$ V (vs NHE and based on a 1 M standard state for aqueous NO). Outside the standard conditions, the midpoint potential for reaction 27 is equivocal,

(26) Wagman, D. D.; Evans, W. H.; Parker, V. B.; Schumm, R. H.; Halow, I.; Bailey, S. M.; Churney, K. L.; Nuttall, R. L. *J. Phys. Chem. Ref. Data* **1982**, *11*, *Suppl. 2*.
(27) Stanbury, D. M. *Adv. Inorg. Chem.* **1989**, *33*, 69−138.
(28) Koppenol, W. H. *Methods Enzymol.* **1996**, *268*, 7−12.
(29) Benson, S. W.; Nangia, P. S. *J. Am. Chem. Soc.* **1980**, *102*, 2843−2844.
(30) Huthwelker, T.; Peter, T.; Luo, B. P.; Clegg, S. L.; Carslaw, K. S.; Brimblecombe, P. *J. Atmos. Chem.* **1995**, *21*, 81−95.
(31) Park, J.-Y.; Lee, Y.-N. *J. Phys. Chem. A* **1988**, *92*, 6294−6302.
(32) Merényi, G.; Lind, J.; Goldstein, S.; Czapski, G. *J. Phys. Chem. A* **1999**, *103*, 5685−5691.
(33) Olson, L. P.; Bartberger, M. D.; Houk, K. N. *J. Am. Chem. Soc.* **2003**, *125*, 3999−4006.
(34) O'Sullivan, D. W.; Lee, M.; Noone, B. C.; Heikes, B. G. *J. Phys. Chem.* **1996**, *100*, 3241−3247.
(35) Johnson, B. J.; Betterton, E. A.; Craig, D. *J. Atmos. Chem.* **1996**, *24*, 113−119.
(36) (a) Merényi, G.; Lind, J. *Chem. Res. Toxicol.* **1997**, *10*, 1216−1220. (b) Poskrebyshev, G. A. *Russ. J. Phys. Chem.* **1998**, *72*, 151−154.
(37) Schwarz, H. A.; Dodson, R. W. *J. Phys. Chem.* **1984**, *88*, 3643−3647.
(38) Lymar, S. V.; Schwarz, H. A.; Czapski, G. *J. Phys. Chem. A* **2002**, *106*, 7245−7250.

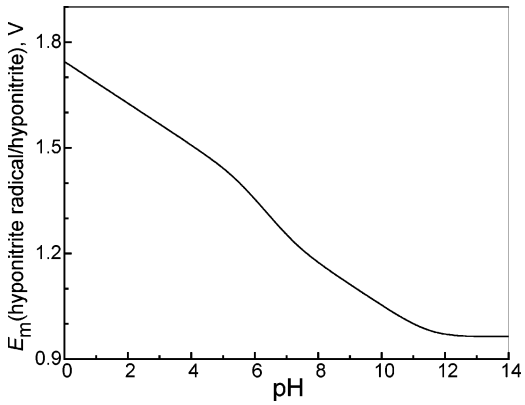

Figure 8. Variation of the midpoint potential (E_m vs NHE) with pH for the one-electron reduction of the hyponitrite radical as in electrode reaction 26. The dependence is calculated using the data in Table 1 and pK_a's of 5.5, 7.2, and 11.5 for HN_2O_2, $H_2N_2O_2$, and $HN_2O_2^-$, respectively. At E_m, $[N_2O_2^-] + [HN_2O_2] = [N_2O_2^{2-}] + [HN_2O_2^-] + [H_2N_2O_2]$.

as it is [NO]-dependent; obviously, the radical will become increasingly more reducing at low [NO]. Because of reactions 24 and 27, the electrochemical oxidation of $N_2O_2^{2-}$ should be irreversible and occur at a potential less positive than $E°(N_2O_2^-/N_2O_2^{2-})$. Consistent with that expectation, an irreversible wave with $E_{1/2} = 0.55$ V (NHE) was reported in a polarographic study.[39]

Discussion

The transient spectrum a in Figure 2 that we have observed and assigned to the hyponitrite radical differs dramatically from the spectrum c reportedly obtained by the addition of NO to the nitroxyl species, as in reaction 2.[5−7] Could this reaction result in a different isomer of the hyponitrite radical than the ON−NO bonded isomers apparently produced by the hyponitrite oxidation and shown in Figures 1 and 7? In a careful isotopic labeling study using ^{15}NO and unlabeled Angeli's salt ($Na_2N_2O_3$) as the source of nitroxyl, Bazylinski and Hollocher[12] have shown that the $^{15}N/^{14}N$ distribution observed in the N_2O product from reactions 2 and 3 occurring seriatim requires that the $N_3O_3^-$ intermediate has a symmetric N−N−N configuration, that is, ON−N(O)−NO$^-$. This result implies that the precursor to $N_3O_3^-$, the $N_2O_2^-$ radical obtained by the NO + HNO/NO$^-$ reaction, already contains the N−N bond. While the ON−NO$^-$ isomer has been experimentally observed in both gas phase[40] and inert matrixes,[41] no ON−ON$^-$ or NO−ON$^-$ isomers have been detected. Furthermore, previous gas-phase calculations for various isomers of HN_2O_2 have shown that the ON−ON and NO−ON species are all (irrespective of the H atom position) not bound and, thus, cannot exist.[24] Although we do compute one bound ON−ONH isomer (Supporting Information note 1), it is ∼70 kJ/mol higher in energy than the ONNOH isomer shown in Figure 7. It is, therefore, unlikely that different HN_2O_2/$N_2O_2^-$ radicals have been produced previously in the pulse radiolysis of NO and in this work.

A more plausible explanation for the disagreement in the $N_2O_2^-$ spectra is that the previously reported spectrum has been misinterpreted and actually belonged to the $N_3O_3^-$ anion. This conjecture is supported by (*i*) the conspicuous similarity of the spectra c and d in Figure 2 previously assigned to $N_2O_2^-$ and $N_3O_3^-$, respectively, (*ii*) practically the same pK_a values of 3.2 and 3.1 previously derived for HN_2O_2 and HN_3O_3, respectively, from the pH dependencies of their absorption intensity,[7] and (*iii*) the recently reported much greater rate of $N_3O_3^-$ formation from $^3NO^-$ than from ^1HNO by the consecutive addition of two NO radicals.[4,11] With respect to the last point, both $^3NO^-$ and ^1HNO should be produced by pulse radiolysis in the NO solutions (from scavenging of e_{aq}^- and H, respectively, by NO). Because $^3NO^-$ generates $N_3O_3^-$ about 400 times faster than does ^1HNO and the protic equilibration between $^3NO^-$ and ^1HNO is slow compared to $N_3O_3^-$ formation,[4,11] a two-step growth of $N_3O_3^-$ optical absorption at 380 nm is expected due to the two processes occurring completely independently

$$^3NO^- + 2NO \rightarrow N_3O_3^- \qquad (28)$$

$$^1HNO^- + 2NO \rightarrow H^+ + N_3O_3^- \qquad (29)$$

These processes should be well separated in time, so that spectra c and d in Figure 2 would appear one after the other, which could have been confused with the transient formation of $N_2O_2^-$. It appears that reexamination of the pulse radiolysis of NO with a higher time resolution than previously available is required to verify this conjecture and reconcile the data; the corresponding work is under way in our laboratories.

Contrary to earlier reports,[5,7] we find the $N_2O_2^-$ radical quite stable both kinetically and thermodynamically with respect to its dissociation (reaction 22), a property that can make this radical a very significant entity in the redox chemistry leading to or originating from NO. Indeed, with the estimated high potential for the reduction of $N_2O_2^-$ (reaction 26) and negative potential for its oxidation (reaction 27), the radical can engage in redox reactions with a number of diverse biological and environmental reductants and oxidants. In addition, the radical is likely to be a good ligand for transition metal ions.

We find that ONNOH is the most stable isomer of the protonated hyponitrite radical (Figure 7 and Supporting Information note 1). Its dissociation could lead to NO + NOH, but not to NO + HNO as shown in reaction 23. Very little is known about the NOH isomer (called hydroxy nitrene); the only observation of NOH was reported in a solid argon matrix at 10 K.[42] Theoretical calculations suggest a triplet ground state for NOH that lies some 80−100 kJ/mol higher in energy than ^1HNO.[43] If so, the dissociation of ONNOH to ^3NOH is impossible, and the only plausible pathway for reaction 23 is

$$ONNOH \leftrightarrows ONN(H)O \leftrightarrows NO + {}^1HNO \qquad (30)$$

The overall reaction 30 is endergonic by only 7 kJ/mol (Table 1), which corresponds to a rather large equilibrium constant of $\sim 6 \times 10^{-2}$ M. Thus, the stability of ONNOH that we observe

(39) Cinquantini, A.; Raspi, G.; Zanello, P. *Anal. Chim. Acta* **1976**, *87*, 51−57.
(40) (a) Posey, L. A.; Johnson, M. A. *J. Chem. Phys.* **1988**, *88*, 5383−5395. (b) Li, R.; Continetti, R. E. *J. Phys. Chem. A* **2002**, *106*, 1183−1189.
(41) (a) Andrews, L.; Zhou, M. F.; Willson, S. P.; Kushto, G. P.; Snis, A.; Panas, I. *J. Chem. Phys.* **1998**, *109*, 177−185. (b) Lugez, C. L.; Thompson, W. E.; Jacox, M. E.; Snis, A.; Panas, I. *J. Chem. Phys.* **1999**, *110*, 10345−10358. (c) Andrews, L.; Zhou, M. F. *J. Chem. Phys.* **1999**, *111*, 6036−6041.
(42) Maier, G.; Reisenauer, H. P.; De Marco, M. *Angew. Chem., Int. Ed.* **1999**, *38*, 108−110.
(43) (a) Luna, A.; Merchán, M.; Roos, B. O. *Chem. Phys.* **1995**, *196*, 437−445. (b) Mordaunt, D. H.; Flöthmann, H.; Stumpf, M.; Keller, H.-M.; Beck, C.; Schinke, R.; Yamashita, K. *J. Chem. Phys.* **1997**, *107*, 6603−6615. (c) Sicilia, E.; Russo, N.; Mineva, T. *J. Phys. Chem. A* **2001**, *105*, 442−450.

is kinetic, not thermodynamic, in nature. Calculations have predicted a very high barrier (~90 kJ/mol) for direct ONNOH to ONN(H)O isomerization through the H atom shift in gas phase.[24,25] Although this barrier is likely to remain in water, an additional isomerization pathway through the intermediacy of the common $ONNO^-$ anion becomes available. However, this deprotonation−protonation pathway should also be significantly activated, for the Gibbs energy of $ONNO^-$ is 31 kJ/mol higher than that of ONNOH (Table 1). The second (dissociation) step in reaction 30 encounters an even larger calculated gas-phase activation barrier of ~40 kJ/mol.[24,25] We conjecture that these activation barriers are collectively responsible for the kinetic stability of ONNOH.

In summary, we have shown that the one-electron oxidation of various protonated forms of hyponitrite by OH, N_3, or SO_4^- generates the hyponitrite radicals ($ONNO^-$ and ONNOH). This radical should also be produced by the additions of nitric oxide to the nitroxyl (^1HNO and $^3NO^-$) species. All the major properties of the hyponitrite radical have been revised, which includes the characteristic radical absorption spectrum, the radical acidity, and the radical stability with respect to dissociation. The radical is found to be both strongly oxidizing and moderately reducing. These revisions suggest that the hyponitrite radical is a potentially important intermediate in the redox chemistry of nitric oxide in biological environments. If previously the reactivities and biochemical effects of nitroxyl and nitric oxide could be considered essentially independently due to the alleged very low stability of their adduct, this investigation shows that the hyponitrite radical formation is a major sink for nitroxyl and that the radical reactivity should be explicitly included in the assessments of the nitroxyl biological roles.

Acknowledgment. We thank Drs. Marshall Newton and Harold Schwarz for insightful comments. Research at Brookhaven National Laboratory was carried out under the auspices of the U.S. Department of Energy under Contract DE-AC02-98CH10886 from the Division of Chemical Sciences, Office of Basic Energy Sciences, and EMPS Grant #73824 (to S.V.L.). Work at New York University was supported by the NIH Grant R01 ES11589 and by a grant from the Kresge Foundation.

Supporting Information Available: Absorption spectra of hyponitrous acid and its anions, concentration dependence of hyponitrite oxidation by azide and sulfate radicals, gas-phase structures and calculated energetics for various isomers of protonated hyponitrite radical, derivation of formation thermodynamic parameters for aqueous hyponitrite species. This material is available free of charge via the Internet at http://pubs.acs.org.

JA038042L